Published in final edited form as:
Hepatology. 2008 September ; 48(3): 909–919. doi:10.1002/hep.22397.

Murine Cirrhosis Induces Hepatocyte Epithelial Mesenchymal Transition and Alterations in Survival Signaling Pathways

Takashi Nitta[*], **Jae-Sung Kim**[*], **Dagmara Mohuczy**, and **Kevin E. Behrns**
Department of Surgery, Division of General and Gastrointestinal (GI) Surgery, University of Florida, Gainesville, FL

Abstract

Hepatocytes that reside in a chronically-injured liver have altered growth responses compared to hepatocytes in normal liver. Transforming growth factor beta (TGFβ) is upregulated in the cirrhotic liver, and cirrhotic hepatocytes, unlike normal hepatocytes exposed to this cytokine, exhibit decreased apoptosis. In fetal hepatocytes, TGFβ also induces epithelial-mesenchymal transition (EMT) and signaling changes in cell survival pathways. Here, chronic murine liver injury was induced by twice-weekly carbon tetrachloride administration for 8 weeks. Normal liver-derived hepatocytes (NLDH) and cirrhotic liver-derived hepatocytes (CLDH) were examined for EMT and the small mothers against decapentaplegic homolog (Smad), phosphatidylinositol-3-kinase (PI3K/Akt), and mitogen activated protein kinase (MAPK) pathways were investigated. Immunofluorescence imaging of cirrhotic livers demonstrated increased vimentin expression, which was confirmed by immunoblot analysis. *In vitro*, CLDH exhibited increased vimentin and type 1 collagen expression within cellular extensions consistent with EMT. Treatment with TGFβ augmented the EMT response in CLDH. In contrast, untreated NLDH did not display features of EMT but responded to TGFβ with increased vimentin expression and EMT characteristics. In response to PI3K/Akt inhibition, CLDH had decreased basal and insulin-stimulated p-Akt expression and decreased apoptosis compared to NLDH. In both NLDH and CLDH, vimentin expression was dependent on PI3K/Akt activity. CLDH demonstrated increased basal p-extracellular signal-regulated kinase expression that was independent of Smad and PI3K/Akt signaling. Inhibition of the MAPK pathway produced a marked increase in CLDH apoptosis. *Conclusion:* CLDH have increased vimentin and type 1 collagen expression and morphologic features consistent with EMT. In addition, compared to NLDH, the cellular signaling phenotype of CLDH changes from a MAPK-independent pathway to a MAPK-dependent cell survival pathway. These findings may have clinical implications for chemoprevention of hepatocellular carcinoma in the cirrhotic liver.

Chronic liver injury is associated with dysregulated growth of hepatocytes and results in the formation of regenerative nodules, dysplastic nodules, and hepatocellular carcinoma. Transforming growth factor beta (TGFβ) expression is increased markedly in the cirrhotic

Address reprint requests to: Kevin E. Behrns, M.D., Department of Surgery, PO Box 100286, 1600 SW Archer Road, Gainesville, FL 32610. Kevin.Behrns@surgery.ufl.edu; fax: 352-265-1060.
[*]These authors contributed equally to this study.

Potential conflict of interest: Nothing to report.

liver and is a potent inducer of stellate cell proliferation and collagen production.[1] In addition, TGFβ induces hepatocyte apoptosis *in vitro*[2] and in the normal liver.[3] However, hepatocytes from a chronically-injured liver exhibit decreased sensitivity to TGFβ-induced apoptosis.[4] The mechanisms by which hepatocytes from a chronically-injured liver resist TGFβ-induced apoptosis and exhibit altered growth control are related, in part, to increased oxidative stress.[4] However, it is likely that several mechanisms are operative in this adaptive change within a chronically inflamed liver. Furthermore, TGFβ expression is also associated with morphologic alterations like epithelial mesenchymal transition (EMT) in fetal[5,6] and adult hepatocytes,[7] and changes in survival signaling pathways,[6] but these cellular events have not been studied in the cirrhotic hepatocytes.

EMT is a dynamic process that has been well-studied in embryonic development[8] and, more recently, has been implicated in the invasion and metastasis phases of carcinogenesis.[9] In addition, substantial investigation of EMT in the chronically-inflamed kidney suggests that this process is responsible for the generation of up to one-third of all fibrotic cells in an inflammatory state.[10] Previous work has demonstrated in a model of fetal hepatocytes that TGFβ treatment induces EMT-like morphologic changes in 50%–60% of the hepatocyte population, whereas the remaining hepatocytes undergo apoptosis.[5,6] In the cells with EMT-like morphology, EMT confers resistance to apoptosis via an epidermal growth factor (EGF)-ligand-dependent mechanism.[5,6] Kaimori et al.[7] recently demonstrated that prolonged exposure of adult mouse hepatocytes to TGFβ increases expression of vimentin and collagen, specific markers of EMT onset, suggesting that hepatocytes may have fibrogenic potential in the liver. Moreover, the Ras/mitogen-activated protein kinase (MAPK) signaling pathway has been implicated in the development of EMT and tumor migration.[11] In a carcinogenic hepatocyte cell line, Raf-1 regulated EMT through activation of extracellular receptor kinase (ERK) with evidence of changes in tight junctions likely mediated through transcriptionally-dependent alterations in occludin and claudin-2 expression.[12] Moreover, in a mammary cell line, phosphatidylinositol-3-kinase (PI3K/Akt) signaling was necessary for EMT and cell migration, an activity that was dependent on RhoA activation.[13] Collectively, these findings suggest that TGFβ induces EMT and that these changes may be mediated through the PI3K/Akt and MAPK pathways, but this hypothesis has not been tested in hepatocytes from a cirrhotic liver.

In addition to morphologic changes, hepatocytes from a cirrhotic liver have altered cell signaling that renders them less susceptible to apoptosis than normal hepatocytes.[4] Decreased sensitivity to apoptosis in cirrhotic hepatocytes appears to be mediated, in part, through a reactive oxygen species (ROS)-dependent mechanism.[4] Chronic liver injury is associated with increased ROS and diseases like hepatitis C result in particularly robust ROS generation.[14] In addition, previous work has demonstrated that TGFβ induces nicotinamide adenine dinucleotide phosphate, reduced form (NADPH) oxidase-like activity, and to a lesser extent, mitochondrial-generated ROS and that oxidative stress is a requirement for TGFβ-induced apoptosis.[15,16] Additional work suggests that the TGFβ-induced ROS activity was inhibited by EGF stimulation that acted through Rac1-dependent and nuclear factor kappa B-dependent mechanisms.[17] Furthermore, the EGF protective mechanism against TGFβ-induced apoptosis may occur through a PI3K/Akt-dependent pathway that preserves

survival in fetal, but not adult hepatocytes.[18] While previous work has demonstrated that Akt interacts directly with mothers against decapentaplegic homolog 3 (Smad3) to induce TGFβ-mediated hepatocyte apoptosis,[19,20] the role of ERK expression in cirrhotic liver-derived hepatocytes (CLDH) apoptosis has not been studied. Taken together, these findings suggest that the PI3K/Akt and MAPK pathways cooperatively regulate hepatocyte proliferation and survival.

Our aim was to determine if CLDH acquire a phenotype consistent with EMT, and if changes in the PI3K/Akt and MAPK pathways correlate with EMT and cell survival. We found that CLDH, in contrast to normal liver-derived hepatocytes (NLDH), exhibited phenotypic and functional changes of EMT and that cell survival was dependent primarily on MAPK.

Materials and Methods

Reagents

All reagents were obtained from Sigma (St. Louis, MO), Fisher Scientific (Fairlawn, NJ), BD (Franklin Lakes, NJ), Calbiochem (La Jolla, CA), Abcam (Cambridge, MA), EMD Biosciences (La Jolla, CA), Chemicon (Temecula, CA), Invitrogen (Carlsbad, CA), Santa Cruz (Santa Cruz, CA), MBL (Woburn, MA), Roche Molecular Biochemicals (Indianapolis, IN), Cell Signaling Technology (CST; Danvers, MA), R&D Systems (Minneapolis, MN), Promega (Madison, WI), or Wako Pure Chemicals (Osaka, Japan).

Animals

Eight-week-old male BALB/c mice (Harlan, Indianapolis, IN) weighing 22 to 25 g were acclimated to a 12-hour light-dark cycle, fed standard chow, and provided water *ad libitum*. All animal procedures and protocols were approved by and in accordance with the University of Florida's Institutional Animal Care and Use Committee. Cirrhosis was induced by administering twice-weekly intraperitoneal injections in a 1:1 mixture of carbon tetrachloride (CCl_4; 1,600 mg/kg; Sigma Aldrich) and sterile mineral oil (Sigma Aldrich) of 2 mL/kg for a total of 8 weeks as described.[4] Control animals received an identical volume of mineral oil. All experiments were performed one week after the final dose of CCl_4.

Primary Hepatocyte Isolation and Culture

NLDH and CLDH were isolated by a two-step collagenase perfusion method.[4] Briefly, mice were anesthetized with mixture of ketamine (Phoenix Scientific, St. Joseph, MO; 105 mg/kg) and xylazine (Phoenix Scientific; 10.5 mg/kg) by intraperitoneal injection. After the animals were anesthetized, through a midline laparotomy, the inferior vena cava was cannulated with an 18G angiocatheter. The portal vein was immediately transected for outflow and the suprahepatic vena cava was clamped. The liver was perfused *in situ* with oxygenated Krebs ringer (4-(2-hydroxyethyl)-1-piperazine ethanesulfonic acid) (HEPES) (KRH) buffer containing 0.5 mM ethylene glycol tetraacetic acid, 115 mM NaCl, 5 mM KCl, 1 mM $MgSO_4$, and 25 mM HEPES (pH 7.4) at 37°C for 5 minutes at 4 mL/minute. Following this liver flush, a nonrecirculating *in vivo* collagenase perfusion with oxygenated KRH buffer (115 mM NaCl, 5 mM KCl, 1 mM $CaCl_2$, and 25 mM HEPES) containing

0.01% collagenase D (Sigma Aldrich) was performed at 37°C for 15 minutes at 4 mL/minute. The harvested liver was minced gently in KRH buffer containing 10 mg/mL bovine serum albumin fraction V (Sigma Aldrich) and filtered with polyamide mesh (I 003 Y NYTEX 3–60/45; TETKO Inc, New York, NY). Hepatocytes were washed twice and centrifuged at 30*g* for 1 minute followed by centrifugation at 30*g* for 2 minutes at 4°C. Cell viability was consistently greater than 88% as determined by trypan blue staining and microscopic counting. Cells were plated on collagen-1 coated glass cover slips, six-well plates, or 60-mm culture dishes in Waymouth's medium containing 10% fetal bovine serum, 100 nM insulin, 0.1 μM dexamethasone, and penicillin/streptomycin. For immunofluorescence staining or immunoblots of type 1 collagen, some hepatocytes were plated on laminin-coated coverslips or culture dishes, and incubated in Waymouth's medium. After 2 hours, the cells were washed with phosphate-buffered saline (PBS; 2.7 mM KCl, 137 mM NaCl 10.1 mM Na_2HPO_4, and 1.8 mM KH_2PO_4, pH 7.4), and the medium was changed to hormonally defined medium (HDM) containing 100 nM insulin, 1 μg/mL apo-transferrin, 0.3 nM sodium selenite, 1.5 μM free fatty acid, and penicillin/streptomycin in Roswell Park Memorial Institute 1640 basal medium.

Primary Hepatocyte Treatment

Primary hepatocytes were cultured in serum-free HDM for 12 hours and pretreated for 1 hour with the PI3K inhibitor, LY294002 (2-(4-Morpholinyl)-8-phenyl-4H-1-benzopyran-4-one) (0–50 μM; CST) or the MEK1/2 inhibitor, U0126 (1,4-diamino-2,3-dicyano-1,4-bis(2-aminophenylthio)butadiene) (0–50 μM; Promega) prior to the administration of TGFβ (5 ng/mL; R&D). A TGFβ concentration of 5 ng/mL was used in all experiments. In experiments with adenoviral infection, hepatocytes were exposed to adenoviruses expressing Smad7 (Ad.Smad7) or a control virus, luciferase (Ad.Luc), at a multiplicity of infection of 10 for 24 hours prior to TGFβ treatment.

Western Blot Analysis

Whole-cell extracts were prepared using lysis buffer (150 mM NaCl, 50 mM Tris-HCl, 1 mM ethylenediaminetetraacetic acid, 1% Triton X-100, 1% sodium deoxycholic acid, 0.1% sodium dodecylsulfate, pH 7.4) with proteinase inhibitor cocktail and phosphatase inhibitor cocktail (Sigma-Al-drich). Protein concentrations were determined by the bicinchoninic acid protein quantification kit (Pierce Biotechnology, Rockford, IL) and reduced with a sample buffer containing 50 mM Tris-HCl, 12.5% glycerol, 1% sodium dodecylsulfate, 0.01% bromophenol blue, and 5% β-mercaptoethanol, with a pH of 6.8 at 95°C for 5 minutes. Protein samples of 25 μg were electrophoresed in a 10% polyacrylamide gel with XCell Surelock System (Invitrogen) and transferred electrophoretically to a 0.2-μm nitrocellulose membrane (Watman GmbH, Dassel, Germany) following the manufacturer's instructions. The membrane was blocked with 5% nonfat milk in Tris-buffered saline Tween-20 (TBS-T: 25 mM Tris HCl, 144 mM NaCl, 0.1% Tween-20, pH 7.4) at room temperature for 1 hour and subsequently incubated with primary antibody at 4°C overnight. The primary antibodies for β-actin (1:2000; Sigma Aldrich) and phospho-Smad2 (CST; Ser465/467, 1:1000) were diluted with 5% nonfat dry milk in TBS-T. All other primary antibodies were diluted in 5% bovine serum albumin in TTBS. This includes anti-vimentin (MBL), anti-collagen (Calbiochem), anti-occludin (ZYMED), anti-E-cadherin (Takara), anti-phospho-Erk1/2 (Thr

202/Tyr 204), anti-phospho-Akt (Ser 473), and anti-phospho-Smad3 (Ser423/425)/Smad1 (Ser463/465). These primary antibody concentrations were 1:1000. The membrane was washed three times with TBS-T at room temperature for 5 minutes each. The membrane was then incubated with horseradish peroxidase conjugated secondary antibody (Santa Cruz Biotechnology; 1:25,000 dilution in TBS-T) at room temperature for 45 minutes and washed three times with TBS-T for 10 minutes each. Signals were detected using the Advanced Chemiluminescence Detection Kit (Amersham Life Sciences, Arlington Heights, IL).

Fluorescence Labeling of Live Hepatocytes

Primary hepatocytes were cultured in six-well plates and treated, as described above. After 48 hours of treatment, HEPES (pH 7.5; 20 mM) was added to stabilize the pH during microscopic imaging under ambient room air conditions. Hepatocellular nuclei were stained with 10 μM Hoechst 33342 (Sigma Aldrich) for 20 minutes. Subsequently, hepatocytes were incubated with 7.5 μg/mL propidium iodide (Sigma Aldrich) to monitor nuclear morphology. Morphologic nuclear changes including condensation and fragmentation were monitored to evaluate the onset of apoptosis using an Axiovert 200 inverted fluorescence microscope (Carl Zeiss MicroImaging GmbH, Göttingen, Germany).[21] Blue (Hoechst 33342) and red (propidium iodide) fluorescent images were collected and overlay images with phase contrast were generated with PhotoShop (Adobe, San Jose, CA). A minimum of five different fields were examined for nuclear condensation, and the percentage of apoptosis was expressed as the number of apoptotic cells divided by the total number of cells.

Immunofluorescence Staining

Sections for immunofluorescence labeling were obtained by perfusing the liver with ice-cold PBS and embedding tissue sections in paraffin/resin compound (Tissue-Tek, Tokyo, Japan). Cryostat sections (4 μm) were fixed with 4% paraformaldehyde dissolved in PBS for 15 minutes at 4°C and permeabilized with 0.1% Triton X-100 in PBS for 5 minutes at room temperature. For hepatocyte staining, cells were cultured on glass coverslips and fixed with 3.7% paraformaldehyde for 10 minutes at room temperature. Samples were blocked with 5% goat serum diluted with PBS including 0.1% Tween-20 for 1 hour and were incubated overnight with anti-vimentin rabbit-antibody (MBL; 1:100 dilution), anti-collagen rabbit antibody (Calbiochem; 1:50 dilution) or anti-albumin rabbit antibody (Abcam; 1:50 dilution) at 4°C. After washing three times with PBS, samples were incubated with a secondary antibody conjugated with a green fluorescing Alexa Fluor 488 (Invitrogen) for 30 minutes at room temperature to visualize vimentin or albumin. Some hepatocytes were costained with Hoechst 33342 in PBS (10 μM) and Alexa Fluor 546-conjugated phalloidin in methanol (330 nM; Invitrogen) at room temperature for 30 minutes to visualize nuclei and F-actin, respectively. Fluorescence of liver sections was imaged with IX-71 fluorescence microscope (Olympus, Center Valley, PA). Hepatocellular images of vimentin (green), collagen (green), and F-actin (red) were collected by using an inverted Zeiss 510 NLO laser scanning confocal microscope equipped with a 63× N.A. 1.4 oil-immersion planapochromat lens. Green and red flu-orophores were excited with 488-nm and 543-nm light, respectively. Emission was divided by a 545-nm dichroic mirror directed through 500 to 530 band-pass and 560-nm long-pass red barrier filters. Pinholes were set to Airy units of 1.0 in both

channels. Nuclei labeled with Hoechst 33342 (blue) were imaged in a multiphoton mode (Chameleon XR; Coherent, Santa Clara, CA) with excitation at 780 nm and emission at 460 nm.

Data Analysis

All experiments were representative of at least three different cell isolations and liver preparations from different mice. Data are expressed as the mean ± standard error of the mean. Statistical significance was assessed with analysis of variance with Bonferroni analysis where appropriate. A *P* value of 0.05 was considered significant.

Results

Previous work[5,6] suggested that fetal hepatocytes exposed to TGFβ underwent EMT that conferred resistance to apoptosis. To investigate whether the TGFβ-rich cirrhotic, adult liver develops EMT, tissue sections of both control and cirrhotic livers were examined by immunofluorescence microscopy for the expression of vimentin, a marker of EMT.[5] The cirrhotic liver demonstrated substantial expression of vimentin predominantly in hepatocytes, whereas, in control liver, expression of vimentin was minimal and limited to the perisinusoidal area (Fig. 1A). Furthermore, liver lysates from cirrhotic mice showed an increased expression of vimentin as compared to lysates from control mice (Fig. 1B). To investigate if hepatocytes develop EMT-like morphology after TGFβ treatment, NLDH and CLDH were treated with or without TGFβ and time-lapse images were collected at 0, 6, 12, and 24 hours using a transmitted light microscope (Fig. 2A). In the absence of TGFβ, morphology of NLDH remained unchanged for 24 hours. However, prolonged exposure to TGFβ in NLDH changed the hepatocyte shape from polygonal to a fibroblast-like phenotype, although many cells lost viability after 24 hours. In contrast to NLDH, many CLDH had an elongated shape even before TGFβ treatment. A fibroblast-like morphology was evident after 6 hours of incubation in the presence or absence of TGFβ treatment. To further examine EMT, the expression of vimentin was determined. Immunoblot analysis demonstrated that basal expression of vimentin (0 hour) in CLDH was substantially higher than in NLDH (Fig. 2B, top panels). Expression of vimentin in the absence of TGFβ remained unchanged in both cells during 24 hours of incubation. When hepatocytes were exposed to TGFβ, vimentin expression was increased both in NLDH and in CLDH. In NLDH, increased expression of vimentin was observed after 6 hour of TGFβ treatment, whereas in CLDH, increased expression of vimentin was evident after 12 hours (Fig. 2B, middle panels). To visualize enhanced expression of vimentin in CLDH, hepatocytes were coimmunostained with F-actin (red) and vimentin (green) after 24 hours of incubation. In NLDH, F-actin localized in the cell to cell junction and in periplasma membrane, a result similar to a previous study[7] (Fig. 2C). Polarization of F-actin was observed when NLDH were treated with TGFβ. Interestingly, compared to NLDH, untreated CLDH had spindle-shaped cellular extensions with prominent vimentin expression at the origin of the extension and at its tip. In CLDH, TGFβ augmented further expression of vimentin throughout the cell. Collectively, these findings suggest that hepatocytes chronically exposed to increased TGFβ in a cirrhotic liver undergo morphologic changes consistent with an EMT phenotype.

Because cirrhotic hepatocytes have decreased sensitivity to apoptotic stimuli and previous evidence suggests that the PI3K/Akt pathway mediates EMT,[13] the anti-apoptotic PI3K/Akt pathway was examined.[19] Insulin is a hepatocellular mitogen that activates the PI3K/Akt pathway, and, therefore, the response of these cells to various concentrations of insulin was determined after 16–18 hour incubation (Fig. 3A). NLDH demonstrated robust phosphorylation of Akt with insulin treatment, but CLDH had little p-Akt expression in the unstimulated state and increased concentrations of insulin resulted in modest Akt phosphorylation as compared to NLDH. Cell viability in both cells was not affected by 100 nM insulin (data not shown) and p-Akt expression declined at higher concentrations of insulin in CLDH (Fig. 3A). Next, we investigated the time-course effect of 100 nM insulin on Akt phosphorylation. In CLDH, rapid Akt phosphorylation occurred within 5 minutes after insulin treatment, but the response was diminished and not sustained when compared to NLDH (Fig. 3B), suggesting that cellular response of Akt to insulin is different between NLDH and CLDH.

To examine the role of PI3K/Akt pathway in TGFβ-mediated apoptosis, NLDH and CLDH were incubated with LY294002, a PI3K inhibitor. Although higher concentrations of LY294002 (>50 μM) completely blocked the expression of p-Akt in both cell types (Fig. 4), the dose-response experiments showed hepatotoxicity at the concentrations higher than 25 μM (data not shown). Thus, we used 25 μM LY294002 throughout the experiments. Densitometric analysis revealed that 25 μM LY294002 blocked p-Akt expression in CLDH, while in NLDH, this concentration decreased p-Akt expression by 30%, compared to its basal state (Fig. 4A) (Image J; National Institutes of Health, Bethesda, MD). Moreover, expression of other proteins including p-ERK1/2, p-BAD, p-P38, and glycogen synthase kinase was not affected by 25 μM LY294002 (data not shown); thus, LY294002 appeared specific for Akt at this concentration. In NLDH, either TGFβ treatment alone or inhibition of PI3K/Akt alone significantly increased apoptosis ($P = 0.0003$) (Fig. 3C,D). However, in the presence of LY294002, TGFβ did not further increase apoptosis ($P = 0.215$). Similar to NLDH, PI3K/Akt inhibition alone, significantly increased apoptosis in CLDH ($P = 0.0002$). In contrast to NLDH, administration of TGFβ to LY294002-treated CLDH further increased apoptosis ($P = 0.027$). These results suggest that factors other than PI3K/Akt may be contributing to CLDH survival.

To further study survival signaling pathways in these cells, we examined the MAPK pathway and the interaction between this pathway and the Smad and PI3K/Akt pathways. CLDH demonstrated increased p-ERK expression compared to NLDH under basal conditions (Fig. 4A). Phosphorylation of ERK was diminished significantly with increasing concentrations of U0126, a MAPK inhibitor, but PI3K/Akt inhibition did not alter p-ERK expression. Since TGFβ signal transduction is mediated through the Smad pathway[20] that is modulated by PI3K/Akt signaling,[22,23] Smad signaling was examined in NLDH and CLDH with or without PI3K/Akt inhibition. CLDH consistently exhibited nonsustained *p*-Smad2 expression 6 hours following treatment with TGFβ (Fig. 4B). This expression pattern was not evident for p-Smad3, but both p-Smad2 and p-Smad3 had decreased expression in response to PI3K/Akt inhibition (Fig. 4B). Because p-Smad2 expression decreased 6 hours following treatment and MAPK signaling may also alter Smad protein expression,[6,24–26]

Smad signaling was examined in the context of PI3K/Akt and ERK expression. At the 6-hour time point after TGFβ treatment, both p-Smad2 and p-Smad3 expression were altered by PI3K/Akt, but not by MAPK inhibition (Fig. 4C). In addition, the PI3K/Akt pathway signaling is not altered by MAPK inhibition. To further assess these cell signaling pathways, NLDH and CLDH were infected with an adenovirus expressing Smad7 (Ad.Smad7) or a control adenovirus and treated with TGFβ. As expected, overexpression of Smad7 inhibited Smad2 and Smad3 expression in both cell types. In addition, overexpression of Smad7 decreased p-Akt expression with or without TGFβ treatment in NLDH and CLDH, with more robust inhibition in NLDH. ERK expression was not altered by Smad7. These findings are consistent with the findings in Fig. 4A–C as well as previous work.[22,23] Interestingly, pretreatment with the antioxidant, Trolox, had no effect on these cell signaling pathways (data not shown) and previous work established that nuclear factor kappa B signaling is not altered in CLDH.[4]

To further assess the PI3K/Akt and MAPK pathways in TGFβ-induced EMT in NLDH and CLDH, vimentin, E-cadherin, and occludin expression were examined in the presence of PI3K/Akt and ERK inhibition (Fig 5A,B). In both cell types, inhibition of the PI3K/Akt pathway for 24 hours decreased vimentin expression following TGFβ treatment (Fig. 5A,B). However, the organization of vimentin and cellular elongation were not altered by treatment with LY294002. U0126 did not affect vimentin expression, the organization of vimentin and cellular elongation in response to TGFβ treatment in either NLDH or CLDH. These findings suggest that the PI3K/Akt pathway, but not the MAPK pathway, is necessary for a late increase in vimentin expression in both cell types.

To examine if CLDH acquire a mesenchymal defining function, the expression of type 1 collagen was evaluated by immunoblots (Fig. 6A) and immunofluorescence analysis (Fig. 6B). In NLDH, collagen expression was barely detectable in the presence or absence of TGFβ. On the contrary, substantial expression of collagen was observed in CLDH under basal conditions. Administration of TGFβ induced a slight increase in collagen expression after 24 hours (Fig. 6A). Immunofluorescence staining of type 1 collagen confirmed enhanced expression of collagen in CLDH that predominantly localized in the periplasma membranes (Fig. 6B). Taken together, these results strongly suggest that CLDH have both EMT-like appearance and EMT-defining function. Next, both NLDH and CLDH were immunostained with albumin to investigate the cellular origin of EMT (Fig. 6C). Confocal imaging of albumin revealed that much like NLDH, nearly all CLDH were positively stained with albumin with or without TGFβ, indicating that these cells are hepatocytes.

To determine the importance of the MAPK pathway on hepatocyte survival, NLDH and CLDH were pre-treated with U0126 and apoptosis was determined. Inhibition of the MAPK pathway had little effect on apoptosis in NLDH with or without TGFβ treatment ($P = 0.105$) (Fig. 7A,B). However, U0126 treatment of CLDH significantly increased apoptosis in cells treated with TGFβ (P italic>0.001). These findings suggest that the MAPK pathway is critically important for CLDH survival in the presence of TGFβ.

Discussion

Cirrhotic livers exhibit a propensity to abnormal hepatocyte growth with the formation of nodules that may harbor dysplastic or carcinoma cells. The cellular and molecular features that permit normally cell-cycle quiescent hepatocytes to proliferate are unknown. In this study we examined changes in hepatocyte cell morphology and growth control signaling pathways to determine potential mechanisms underlying the significant changes in hepatocyte morphology and function in a chronically-injured liver. This study revealed several important distinct characteristics of hepatocytes that reside in a cirrhotic liver. First, CLDH exhibit cell morphology consistent with EMT, more specifically, increased vimentin expression and decreased E-cadherin and occludin expression. Second, CLDH have EMT-defining function since these cells produce type-1 collagen, a key molecule mediating liver fibrosis. Furthermore, the PI3K/Akt pathway appears to mediate changes in vimentin expression. In addition, in contrast to NLDH, which are dependent on the PI3K/Akt pathway for survival, CLDH are dependent on enhanced MAPK signaling for survival. These findings suggest that CLDH undergo morphologic and molecular changes and resistance to apoptosis that may lead to hepatocarcinogenesis.

EMT is a process that is normally evident in embryonic stages of development and recently has been investigated as a mechanism of cancer cell migration and metastasis.[9,27] In addition, studies in chronic fibrotic renal disease have demonstrated that a substantial proportion of the fibroblasts originate from EMT via tubular epithelial cells.[28] Previously, the requirement of Smad-dependent transcription for TGFβ-induced EMT has been shown in chronic renal injury.[29] In the liver, no *in vivo* evidence exists to substantiate EMT in a model of chronic injury. However, a subpopulation of fetal hepatocytes, when exposed to TGFβ *in vitro*, resist apoptosis and demonstrate morphologic features and protein expression markers of EMT.[5] Importantly, these fetal hepatocytes that demonstrated features of EMT had increased expression of p-Akt and Bcl-xl, but ERK expression was decreased compared to fetal hepatocytes treated with TGFβ. The findings in the current study show that p-Akt is required for increased vimentin expression consistent with EMT, but changes in Bcl-xl expression were not evident (data not shown). These findings are consistent with previous work in non-hepatocyte cell lines that demonstrate the importance of the PI3K/Akt signaling in EMT.[10]

Even though the PI3K/Akt pathway enhances vimentin expression in this model, this signal transduction pathway heretofore has not been viewed as a major regulator of classic EMT.[10] The PI3K/Akt pathway may be involved in an *in vitro* EMT-like process, “reversible scatter,” in which cells adopt a spindle-like shape and have a brief period of EMT-related transcriptional activity, neither of which is sustained.[10] Our *in vivo* findings support classic EMT in this model of the chronic liver injury because of increased vimentin expression. However, the role of the PI3K/Akt pathway in the cirrhotic mouse liver appears to differ from that in normal liver. We found that the PI3K/Akt pathway served an important anti-apoptotic function in NLDH, but in CLDH, MAPK integrity was important for hepatocyte survival. Previous work has demonstrated that in NLDH, the PI3K/Akt pathway is critical for proliferation whereas the MAPK pathway is needed for both proliferation and survival.[30] This hypothesis is supported by previous work that demonstrated the antiapoptotic function

of the PI3K/Akt pathway in hepatocytes.[19] The mechanisms by which PI3K/Akt inhibit hepatocyte apoptosis are multiple, but in an acute model of ischemia and reperfusion, primary hepatocytes pretreated with hepatocyte growth factor had activation of PI3K/Akt and subsequent decreased ROS and apoptosis.[31] This model is in contrast to our findings in CLDH, which have chronically increased basal ROS, decreased basal and insulin-stimulated p-Akt, and decreased responsiveness to TGFβ-induced apoptosis. In summary, these findings suggest that CLDH differ significantly from NLDH in cell protective signaling pathways with the MAPK pathway serving as the predominant cell survival pathway in CLDH.

In contrast to the PI3K/Akt pathway that has not been viewed as a significant modulator of EMT, the EGF receptor family and downstream Raf and MAPK pathways have received considerable investigation, particularly related to cell movement and actin rearrangement.[10] In addition, MAPK and ERK signaling are important for hepatocyte replication, and recent evidence shows that ERK2 is the principal factor involved in normal hepatocyte cell cycle progression.[32] However, cell signaling in CLDH, which have increased basal ROS, may differ significantly from NLDH because oxidative stress has been shown to increase basal ERK phosphorylation.[33] Indeed, our findings show that CLDH survival is dependent on MAPK signaling. Importantly, this work also shows that the PI3K/Akt and MAPK signaling pathways act independently. Previous work has demonstrated synergy between the PI3K/Akt and Smad pathways, but in this study, MAPK signaling was independent of Smad input and therefore likely not the result of TGFβ-induced changes including EMT. Therefore, these data suggest that CLDH undergo phenotypic changes consistent with EMT and have a concomitant, but TGFβ-independent, necessity for MAPK signaling.

One of the key findings in the present study is that CLDH not only have EMT-like appearance but have capability of synthesizing type 1 collagen, a molecule that mediates liver fibrosis. Although potential involvement of hepatocytes in collagen production has been suggested in the past,[34] it is generally thought that hepatic fibrosis is the result of collagen production by hepatic stellate cells.[35] Our results show that chronic exposure to TGFβ induces the transition of hepatocytes to collagen-producing mesenchymal cells. Furthermore, immunostaining with albumin demonstrate that CLDH are indeed hepatocytes, although they exhibit morphological and functional characteristics of mesenchymal cells. Our findings are in agreement with a recent study in which prolonged exposure of hepatocytes to TGFβ increases the expression of collagen and induces cytoskeletal rearrangement that resembles EMT.[7] Therefore, the present study suggests that hepatocytes may be a contributor to hepatic fibrosis, especially when they are chronically injured.

Collectively, the findings in this study suggest that in an environment of chronic inflammation and fibrosis with increased TGFβ expression, hepatocytes undergo distinct phenotypic, functional and cell signaling changes that promote cell survival. These morphologic and molecular alterations may provide the foundation for hepatocarcinogenesis. Moreover, better understanding of the cellular and molecular characteristics of the cirrhotic hepatocyte may permit the development of chemopreventative agents for hepatocellular carcinoma.

Acknowledgments

Supported by U.S. Public Health Service (USPHS) grant R01DK066211 (to K.E.B.) from the National Institute of Diabetes and Digestive and Kidney Diseases (NIDDK).

Abbreviations

CLDH	cirrhotic liver-derived hepatocytes
EGF	epidermal growth factor
EMT	epithelial mesenchymal transition
ERK	extracellular receptor kinase
HDM	hormonally defined medium
HEPES	[4-(2-hydroxyethyl)-1-piperazine ethanesulfonic acid]
Smad	small mothers against decapentaplegic homolog
KRH	Krebs ringer HEPES
MAPK	mitogen activated protein kinase
MEK	mitogen activated or extracellular signal-regulated protein kinase
NLDH	normal liver-derived hepatocytes
PBS	phosphate-buffered saline
PI3K/Akt	phosphatidylinositol-3-kinase
Ras	rat sarcoma oncogene
RhoA	Ras homolog gene family member A
Rac1	Ras-related C3 tobulinum toxin substrate 1
ROS	reactive oxygen species
TBS-T	Tris-buffered saline Tween-20
TGFβ	transforming growth factor beta

References

1. Eghbali-Fatourechi G, Sieck GC, Prakash YS, Maercklein P, Gores GJ, Fitzpatrick LA. Type I procollagen production and cell proliferation is mediated by transforming growth factor-beta in a model of hepatic fibrosis. Endocrinology. 1996; 137:1894–1903. [PubMed: 8612529]
2. Oberhammer FA, Pavelka M, Sharma S, Tiefenbacher R, Purchio AF, Bursch W, et al. Induction of apoptosis in cultured hepatocytes and in regressing liver by transforming growth factor beta 1. Proc Natl Acad Sci U S A. 1992; 89:5408–5412. [PubMed: 1608949]
3. Schrum LW, Bird MA, Salcher O, Burchardt ER, Grisham JW, Brenner DA, et al. Autocrine expression of activated transforming growth factor-beta(1) induces apoptosis in normal rat liver. Am J Physiol Gastrointest Liver Physiol. 2001; 280:G139–G148. [PubMed: 11123207]
4. Black D, Bird MA, Samson CM, Lyman S, Lange PA, Schrum LW, et al. Primary cirrhotic hepatocytes resist TGFbeta-induced apoptosis through a ROS-dependent mechanism. J Hepatol. 2004; 40:942–951. [PubMed: 15158334]

5. Valdes F, Alvarez AM, Locascio A, Vega S, Herrera B, Fernandez M, et al. The epithelial mesenchymal transition confers resistance to the apoptotic effects of transforming growth factor Beta in fetal rat hepatocytes. Mol Cancer Res. 2002; 1:68–78. [PubMed: 12496370]
6. Del CG, Murillo MM, varez-Barrientos A, Bertran E, Fernandez M, Sanchez A, et al. Autocrine production of TGF-beta confers resistance to apoptosis after an epithelial-mesenchymal transition process in hepatocytes: Role of EGF receptor ligands. Exp Cell Res. 2006; 312:2860–2871. [PubMed: 16828470]
7. Kaimori A, Potter J, Kaimori JY, Wang C, Mezey E, Koteish A. Transforming growth factor-beta1 induces an epithelial-to-mesenchymal transition state in mouse hepatocytes in vitro. J Biol Chem. 2007; 282:22089–22101. [PubMed: 17513865]
8. Hay ED. An overview of epithelio-mesenchymal transformation. Acta Anat (Basel). 1995; 154:8–20. [PubMed: 8714286]
9. Thompson EW, Newgreen DF, Tarin D. Carcinoma invasion and metastasis: a role for epithelial-mesenchymal transition? Cancer Res. 2005; 65:5991–5995. [PubMed: 16024595]
10. Kalluri R, Neilson EG. Epithelial-mesenchymal transition and its implications for fibrosis. J Clin Invest. 2003; 112:1776–1784. [PubMed: 14679171]
11. Huber MA, Kraut N, Beug H. Molecular requirements for epithelial-mesenchymal transition during tumor progression. Curr Opin Cell Biol. 2005; 17:548–558. [PubMed: 16098727]
12. Lan M, Kojima T, Osanai M, Chiba H, Sawada N. Oncogenic Raf-1 regulates epithelial to mesenchymal transition via distinct signal transduction pathways in an immortalized mouse hepatic cell line. Carcinogenesis. 2004; 25:2385–2395. [PubMed: 15308585]
13. Bakin AV, Tomlinson AK, Bhowmick NA, Moses HL, Arteaga CL. Phosphatidylinositol 3-kinase function is required for transforming growth factor beta-mediated epithelial to mesenchymal transition and cell migration. J Biol Chem. 2000; 275:36803–36810. [PubMed: 10969078]
14. Raval J, Lyman S, Nitta T, Mohuczy D, Lemasters JJ, Kim JS, et al. Basal reactive oxygen species determine the susceptibility to apoptosis in cirrhotic hepatocytes. Free Radic Biol Med. 2006; 41:1645–1654. [PubMed: 17145552]
15. Carmona-Cuenca I, Herrera B, Ventura JJ, Roncero C, Fernandez M, Fabregat I. EGF blocks NADPH oxidase activation by TGF-beta in fetal rat hepatocytes, impairing oxidative stress, and cell death. J Cell Physiol. 2006; 207:322–330. [PubMed: 16331683]
16. Herrera B, Murillo MM, Alvarez-Barrientos A, Beltran J, Fernandez M, Fabregat I. Source of early reactive oxygen species in the apoptosis induced by transforming growth factor-beta in fetal rat hepatocytes. Free Radic Biol Med. 2004; 36:16–26. [PubMed: 14732287]
17. Murillo MM, Carmona-Cuenca I, Del CG, Ortiz C, Roncero C, Sanchez A, et al. Activation of NADPH oxidase by transforming growth factor-beta (TGF-beta) in hepatocytes mediates up-regulation of epidermal growth factor (EGF) receptor ligands through a NF-kappaB-dependent mechanism. Biochem J. 2007; 405:251–259. [PubMed: 17407446]
18. Caja L, Ortiz C, Bertran E, Murillo MM, Miro-Obradors MJ, Palacios E, et al. Differential intracellular signalling induced by TGF-beta in rat adult hepatocytes and hepatoma cells: implications in liver carcinogenesis. Cell Signal. 2007; 19:683–694. [PubMed: 17055226]
19. Hatano E, Brenner DA. Akt protects mouse hepatocytes from TNF-alpha-and Fas-mediated apoptosis through NK-kappa B activation. Am J Physiol Gastrointest Liver Physiol. 2001; 281:G1357–G1368. [PubMed: 11705740]
20. Shi Y, Massague J. Mechanisms of TGF-beta signaling from cell membrane to the nucleus. Cell. 2003; 113:685–700. [PubMed: 12809600]
21. Sit KH, Yin L, Paramanantham R. Apoptotic condensations in M-phase cells. Anat Rec. 1997; 248:149–158. [PubMed: 9185980]
22. Conery AR, Cao Y, Thompson EA, Townsend CM Jr, Ko TC, Luo K. Akt interacts directly with Smad3 to regulate the sensitivity to TGF-beta induced apoptosis. Nat Cell Biol. 2004; 6:366–372. [PubMed: 15104092]
23. Remy I, Montmarquette A, Michnick SW. PKB/Akt modulates TGF-beta signalling through a direct interaction with Smad3. Nat Cell Biol. 2004; 6:358–365. [PubMed: 15048128]

24. Kale VP. Differential activation of MAPK signaling pathways by TGF-beta1 forms the molecular mechanism behind its dose-dependent bidirectional effects on hematopoiesis. Stem Cells Dev. 2004; 13:27–38. [PubMed: 15068691]
25. Lee MS, Ko SG, Kim HP, Kim YB, Lee SY, Kim SG, et al. Smad2 mediates Erk1/2 activation by TGF-beta1 in suspended, but not in adherent, gastric carcinoma cells. Int J Oncol. 2004; 24:1229–1234. [PubMed: 15067346]
26. Potempa S, Ridley AJ. Activation of both MAP kinase and phosphatidylinositide 3-kinase by Ras is required for hepatocyte growth factor/scatter factor-induced adherens junction disassembly. Mol Biol Cell. 1998; 9:2185–2200. [PubMed: 9693375]
27. Tarin D, Thompson EW, Newgreen DF. The fallacy of epithelial mesenchymal transition in neoplasia. Cancer Res. 2005; 65:5996–6000. [PubMed: 16024596]
28. Iwano M, Plieth D, Danoff TM, Xue C, Okada H, Neilson EG. Evidence that fibroblasts derive from epithelium during tissue fibrosis. J Clin Invest. 2002; 110:341–350. [PubMed: 12163453]
29. Zeisberg M, Hanai J, Sugimoto H, Mammoto T, Charytan D, Strutz F, et al. BMP-7 counteracts TGF-beta1-induced epithelial-to-mesenchymal transition and reverses chronic renal injury. Nat Med. 2003; 9:964–968. [PubMed: 12808448]
30. Coutant A, Rescan C, Gilot D, Loyer P, Guguen-Guillouzo C, Baffet G. PI3K-FRAP/mTOR pathway is critical for hepatocyte proliferation whereas MEK/ERK supports both proliferation and survival. Hepatology. 2002; 36:1079–1088. [PubMed: 12395317]
31. Ozaki M, Haga S, Zhang HQ, Irani K, Suzuki S. Inhibition of hypoxia/reoxygenation-induced oxidative stress in HGF-stimulated antiapoptotic signaling: role of PI3-K and Akt kinase upon rac1. Cell Death Differ. 2003; 10:508–515. [PubMed: 12728249]
32. Fremin C, Ezan F, Boisselier P, Bessard A, Pages G, Pouyssegur J, et al. ERK2 but not ERK1 plays a key role in hepatocyte replication: an RNAi-mediated ERK2 knockdown approach in wild-type and ERK1 null hepatocytes. Hepatology. 2007; 45:1035–1045. [PubMed: 17393467]
33. Kim SK, Woodcroft KJ, Oh SJ, Abdelmegeed MA, Novak RF. Role of mechanical and redox stress in activation of mitogen-activated protein kinases in primary cultured rat hepatocytes. Biochem Pharmacol. 2005; 70:1785–1795. [PubMed: 16242670]
34. Chojkier M. Hepatocyte collagen production in vivo in normal rats. J Clin Invest. 1986; 78:333–339. [PubMed: 3734095]
35. Friedman SL. Hepatic stellate cells: protean, multifunctional, and enigmatic cells of the liver. Physiol Rev. 2008; 88:125–172. [PubMed: 18195085]

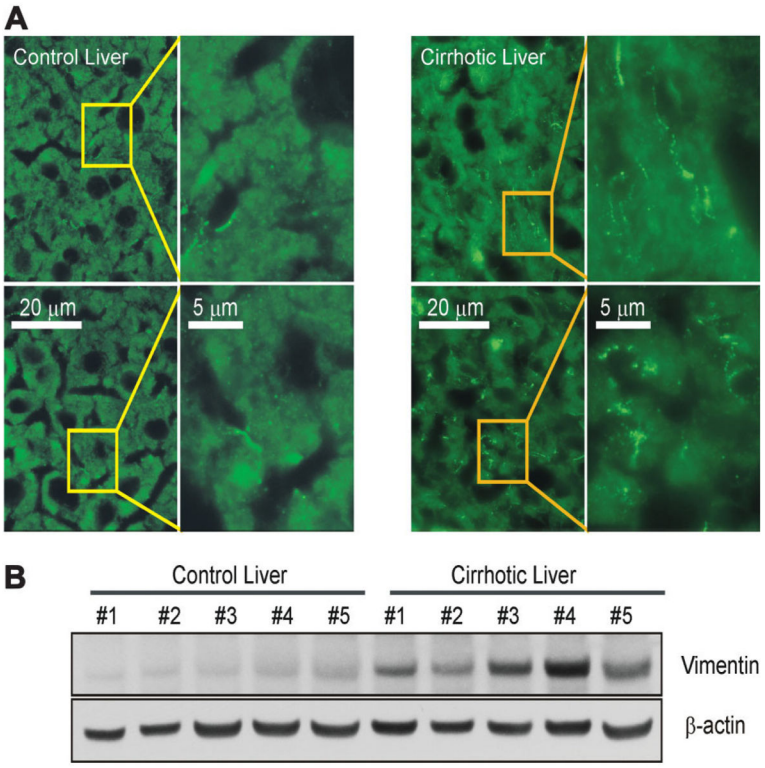

Fig. 1.

Vimentin in cirrhotic livers. (A) Vimentin in normal and cirrhotic mouse livers was visualized by immunofluorescence staining. Each panel represents a separate experiment. Note the characteristic fibrous staining of vimentin in hepatocytes in cirrhotic liver. In contrast, little staining was observed in hepatocytes in control liver. (B) Western blot analysis of liver lysates from control (n = 5) and cirrhotic mice (n = 5). All lysates are from five separate experiments and exhibit overexpression of vimentin in cirrhotic livers.

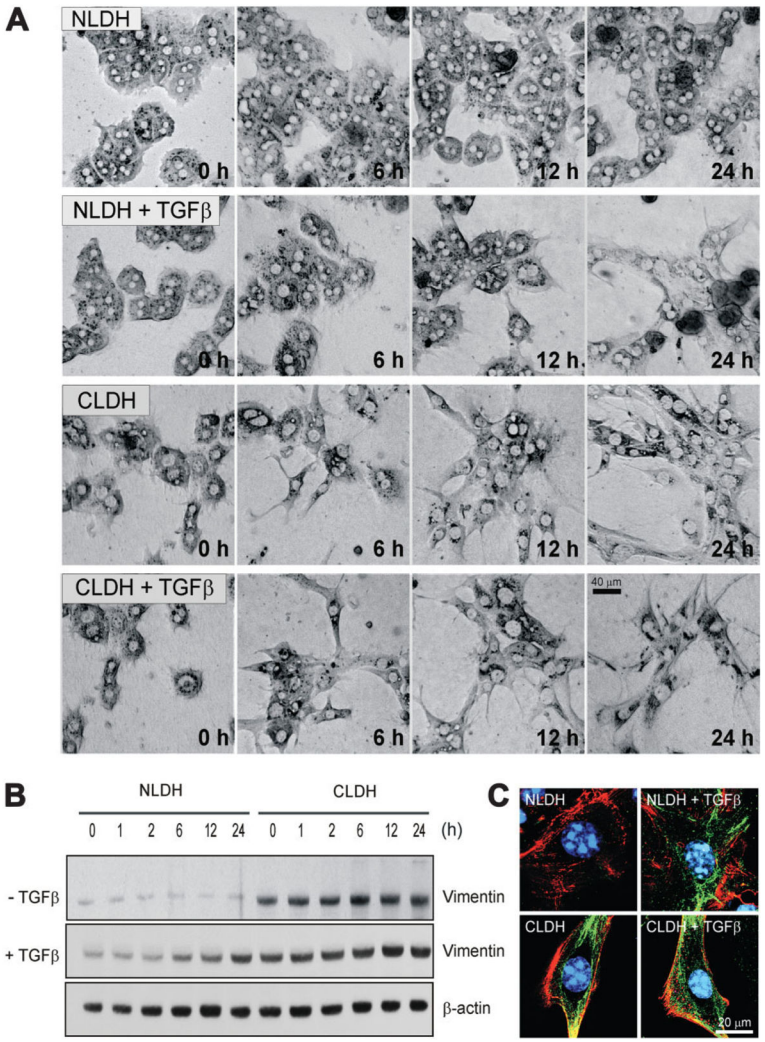

Fig. 2.

Vimentin in primary cultured hepatocytes. (A) Time lapse imaging of hepatocyte morphology changes. Note a fibroblast-like appearance of CLDH in the presence or absence of TGF*β*. (B) Western blot analysis of lysates from primary cultured hepatocytes with or without TGF*β*. CLDH exhibit higher vimentin expression than NLDH before and after TGF*β* treatment. (C) Immunofluorescence microscopy of vimentin. Hepatocytes were costained with vimentin (green), F-actin (red), and Hoechst 33342 (blue) and confocal images were collected. TGF*β* treatment induced the expression of vimentin and EMT morphologically in NLDH, whereas untreated NLDH did not show mesenchymal characteristics. However, even untreated CLDH demonstrated features of EMT. These characteristic were augmented by TGF*β*.

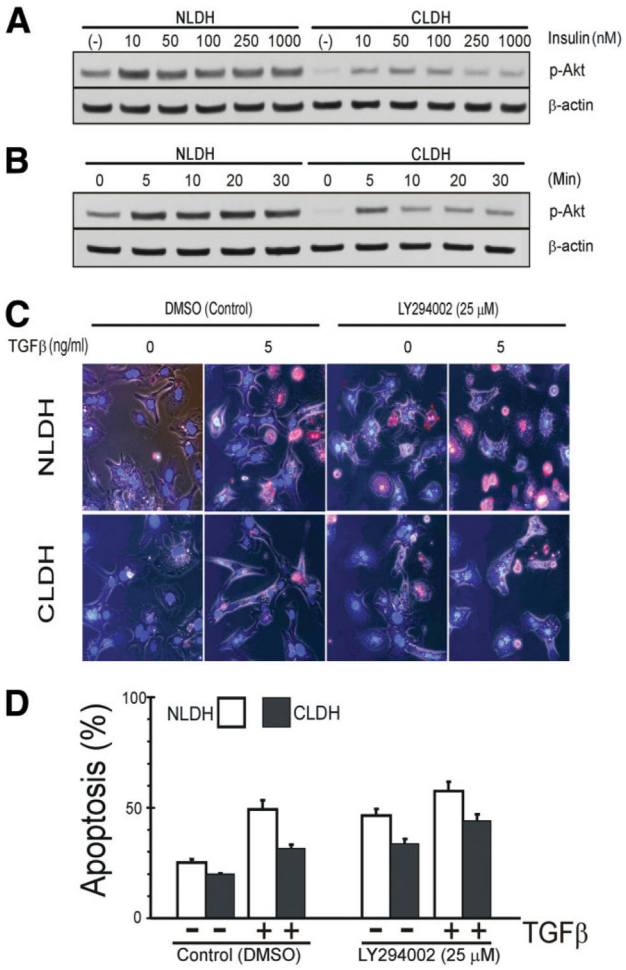

Fig. 3.

Dependence on PI3K/Akt pathway. (A) NLDH and CLDH were incubated 16–18 hours in medium with varying insulin concentrations. In NLDH, p-Akt expression is increased compared to CLDH. Even in the absence of insulin, NLDH maintained higher expression of p-Akt than CLDH. (B) In contrast to NLDH, addition of 100 nM insulin to CLDH did not show sustained expression of p-Akt. (C) Morphologic apoptosis was determined 24 hours after TGFβ stimulation in the presence of PI3K/Akt pathway inhibition. Cell death was evaluated using Hoechst 33342 and propidium iodide (PI). (D) Quantification of apoptosis. Apoptosis was expressed as the percentage of apoptotic cells over total cells. NLDH exhibited a robust increase in apoptotic death by TGFβ treatment, compared to the CLDH (*P* bold> 0.001). Note that CLDH treated with both LY294002 and TGFβ showed a further development of apoptosis, compared to LY294002 or TGFβ alone.

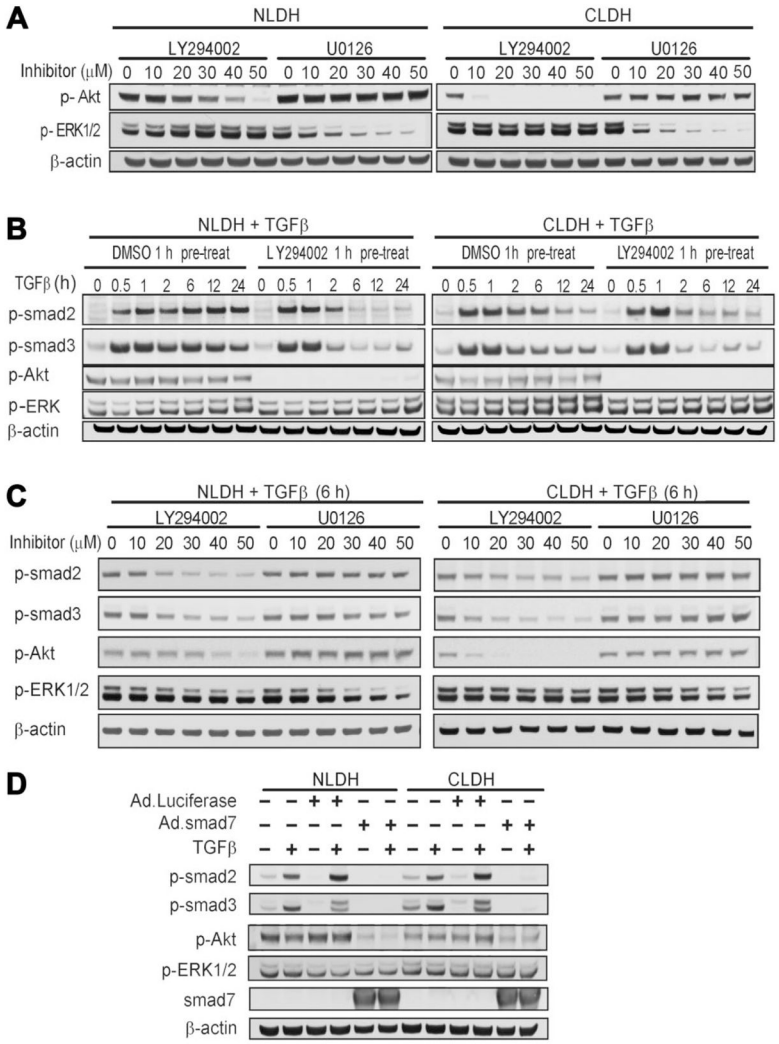

Fig. 4.

The effect of inhibition of the PI3K/Akt and MEK/ERK pathways on the TGF*β* Smad signaling pathway. (A) The PI3K inhibitor, LY294002, decreased p-Akt in both normal and cirrhotic hepatocytes in a dose-dependent manner during 1 hour of treatment. MEK1/2 inhibitor, U0126, decreased p-ERK1/2 in both NLDH and CLDH in a dose-dependent manner. PI3K/Akt and MAPK/ERK signaling demonstrated no interdependence. (B) Time course of Smad signaling response to TGF*β*. Phosphorylation of Smad2/3 induced by TGF*β* was sustained for 24 hours in NLDH. In contrast, CLDH demonstrated decreased p-Smad2 after 2 hours. With LY294002 pretreatment, p-Smad2 was substantially decreased after TGF*β* treatment in both NLDH and CLDH. The initial response of Smad2/3 signal transduction, however, was not affected by LY294002. (C) P-Smad2/3 decreased at 6 hours after TGF*β*1 treatment in NLDH and CLDH in a dose-dependent manner. (D) NLDH and CLDH were infected with adenoviruses expressing Smad7 (Ad.Smad7) or a control protein, luciferase (Ad.Luc), at a multiplicity of infection (MOI) of 10 for 24 hours prior to treatment with TGF*β*. Smad7 over-expression inhibited expression of p-Smad2 and p-Smad3 in both

NLDH and CLDH. In addition, p-Akt expression was decreased markedly in NLDH and modestly in CLDH in response to Smad7 treatment.

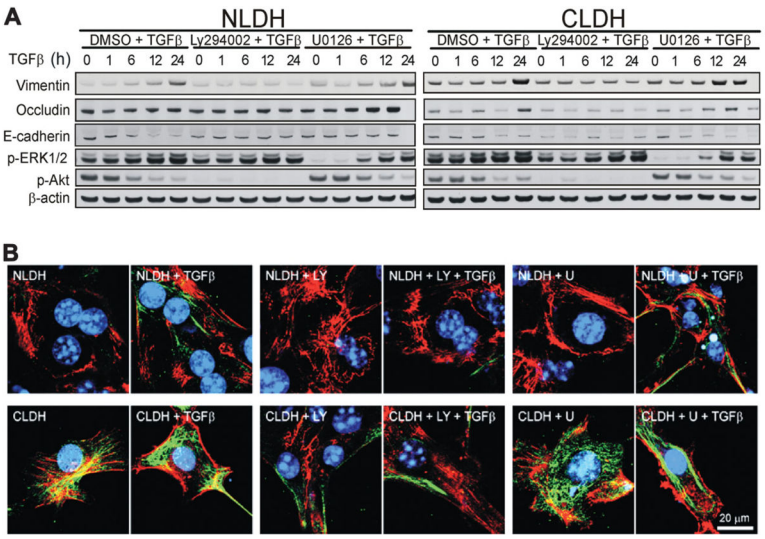

Fig. 5.

The effect of inhibition of the PI3K/Akt and ERK1/2 pathways on EMT after TGF*β* stimulation. (A) NLDH and CLDH were pretreated with LY294002 (25 *μ*M) or U0126 (25 *μ*M) and stimulated with TGF*β*. CLDH showed higher basal expression of vimentin than NLDH, which was further increased after 24 hours of stimulation. NLDH exhibited higher occludin and E-cadherin expression and lower vimentin expression compared to the CLDH consistent with an EMT response. (B) LY294002 (LY) pretreatment suppressed expression of vimentin in both NLDH and CLDH. However, U0126 (U) did not inhibit the expression of vimentin.

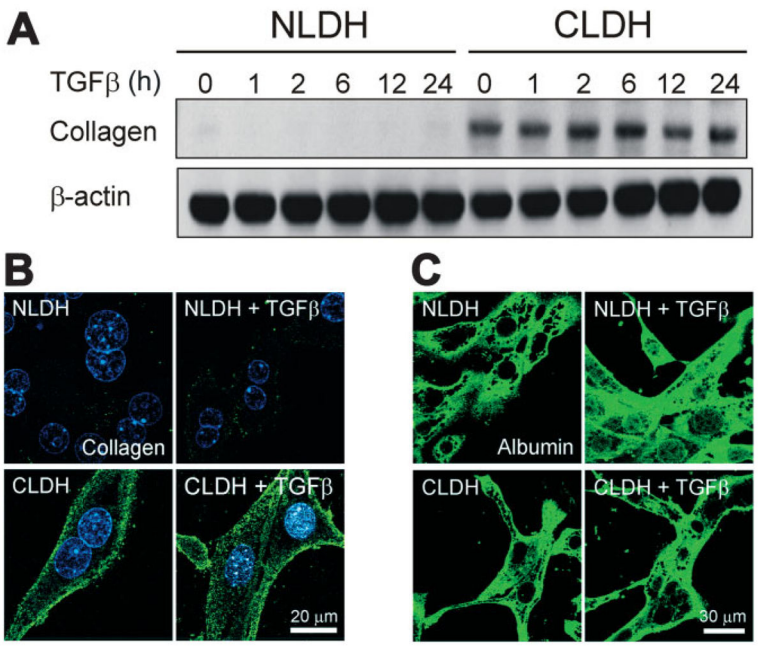

Fig. 6.

Type 1 collagen in primary cultured hepatocytes. (A) Western blot analysis of type 1 collagen showed increased expression of collagen in CLDH. (B) After 24 hours of incubation of both cell types with or without TGF*β*, immunofluorescence images of collagen (green) and Hoechst 33342 (blue) were collected by confocal microscope. (C) After 24 hours of incubation with or without TGF*β*, the expression of albumin, a hepatocyte marker, was assessed by immunofluorescence staining. Note that CLDH were positively stained with albumin despite the morphology representing EMT.

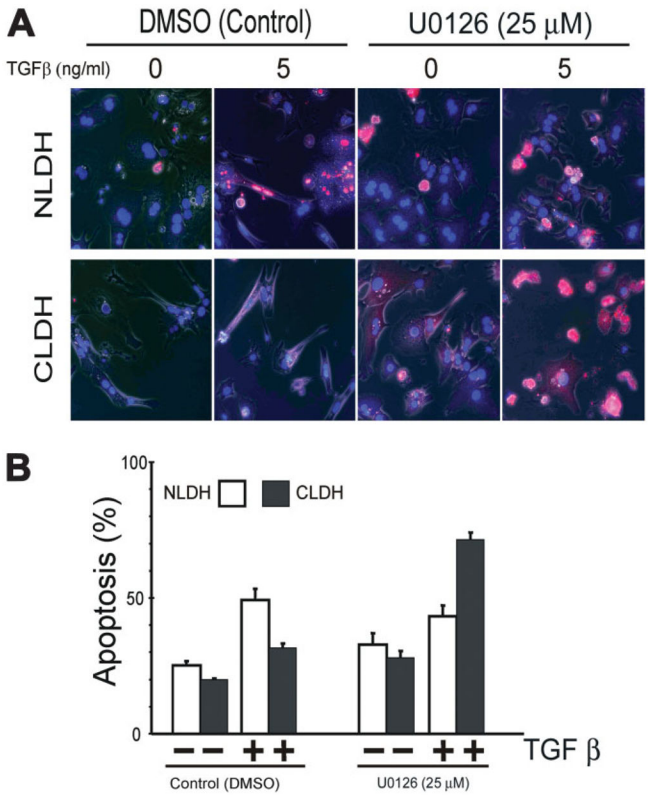

Fig. 7.

The effect of MEK/ERK inhibition on TGFβ-induced apoptosis. (A) Inhibition of MAPK pathway followed by TGFβ treatment induced significant cell death in CLDH. (B) Quantitative analysis of apoptosis from each group. CLDH demonstrated significantly increased apoptosis with MAPK inhibition and TGFβ treatment ($P < 0.001$).